Applied Physics Letters ARTICLE scitation.org/journal/apl

Monitoring the dispersion and agglomeration of silver nanoparticles in polymer thin films using localized surface plasmons and Ferrell plasmons

Cite as: Appl. Phys. Lett. **116**, 103105 (2020); doi: 10.1063/1.5140247
Submitted: 26 November 2019 · Accepted: 27 February 2020 ·
Published Online: 12 March 2020

Rafael C. Hensel,[1] Murilo Moreira,[1] Antonio Riul, Jr.,[1] Osvaldo N. Oliveira, Jr.,[2] Varlei Rodrigues,[1] and Matthias Hillenkamp[1,3,a)]

AFFILIATIONS

[1]Instituto de Física Gleb Wataghin, UNICAMP, 13083-859 Campinas, SP, Brazil
[2]São Carlos Institute of Physics (IFSC), University of São Paulo (USP), P.O. Box 369, 13566-590 São Carlos, SP, Brazil
[3]Institute of Light and Matter, University Lyon, Université Claude Bernard Lyon 1, CNRS, UMR5306, F-69622 Villeurbanne, France

[a)]**Author to whom correspondence should be addressed**: matthias.hillenkamp@univ-lyon1.fr

ABSTRACT

The ability to disperse metallic nano-objects in a given matrix material is an important issue for the design and fabrication of functional materials. A means to monitor the spatial distribution of the nano-dopants is highly desirable but often possible only *a posteriori* and with destructive techniques. Here we present a spectroscopic characterization based on different plasmonic responses of silver nanoparticles, their agglomerates, and finally the percolated silver film. We demonstrate its usefulness for the specific case of their dispersion in layer-by-layer polymeric films but the method is extendable to any other host material transparent in the visible/near UV range. Individual silver nanoparticles display the well-known localized surface plasmon resonance around 400 nm, which is red-shifted upon inter-particle coupling. The transition regime between weakly coupled particles and fully percolated metal films is, however, much harder to evidence unambiguously. We show here how to monitor this transition using the so-called Ferrell plasmon, a plasmonic mode of the thin film in the mid-UV, and excitable only under oblique irradiation but without specific coupling precautions. We can thus follow the entire transition from isolated to coupled and finally to fully agglomerated nanoparticles by optical spectroscopy.

Polymers constitute a large class of soft matter materials with a broad range of properties, playing essential and ubiquitous roles in everyday life. Specifically when fabricated in alternating structures of polyelectrolytes ("Layer-by-Layer," LbL), they represent a valuable toolbox for the high precision fabrication and tuning of properties of thin films through the choice of constituents.[1] LbL is based on the sequential adsorption of polyelectrolytes via electrostatic and non-covalent (van der Waals, hydrogen bonding, hydrophobic, charge-transfer, etc.) interactions, endowing multilayers with distinct functionalities and capabilities to address a wide range of applications. They exist, e.g., as insulators and conductors or with variable optical and mechanical properties such as transparency, stiffness or porosity (i.e., gas permeability).[2,3] The inclusion of metallic aggregates into a polymer matrix has attracted a lot of attention in the last few years as it can significantly enhance its mechanical, optical, thermal, electrical, or catalytic properties,[4–7] but so far this is achieved mainly through chemical approaches. Typically, chemically fabricated and passivated nanoparticles (NPs) are added to the spin-coating solution or used as one of the polyelectrolytes, leaving crucial parameters like particle concentration and interfaces out of reach. The inclusion of physically fabricated, pure metallic NPs in simpler polymers such as polydimethylsiloxane (PDMS), poly(methyl methacrylate) (PMMA) or polystyrene[8] has, however, demonstrated the feasibility and potential use in applications like stretchable electronics,[9] or plasmonic materials,[10] actuators,[11] and antibacterial materials.[12]

One of the most promising applications of thin polymer films with embedded metal NPs is in (bio)sensors. LbL polymer films are widely used as active biocompatible and functionalized layers in sensors based on the impedance response over a large frequency range in combination with data processing methods such as Principal Component Analysis.[13] This multi-dimensional data extraction allows efficient discrimination between trace amounts of different analytes, even in minute quantities. Tuning the impedance of the active layer by controlling the metal loading through NP incorporation is expected to

significantly enhance both sensitivity and selectivity of such devices,[14] as already demonstrated for an LbL system.[15] The underlying mechanisms remain, however, unclear and the study of systems with controlled architecture is needed. Notably, the NP composition (including surface termination), their size, and spatial dispersion inside the polymer matrix are crucial parameters to determine the composite's properties and suitability in applications. In order to better understand the influence of the different parameters, the particles should be isolated from each other. In this case, the well-known and well-defined individual properties, such as the Localized Surface Plasmon Resonance (LSPR) or superparamagnetism, can be exploited, which are otherwise often masked or complicated by inter-particle interactions, e.g., in spin-glasses. This knowledge is crucial to design composite structures for specific applications in sensors, fuel cell membranes, and energy harvesting applications.

The aim of this Letter is to demonstrate how to monitor the spatial dispersion and agglomeration of silver NPs in LbL polymer films using optical spectroscopy. We show how to infer the transition from isolated to coupled NPs and finally to a continuous film from the plasmonic response.

Our approach to fabricating benchmark samples of LbL polymer films with embedded metal NPs is based on the fragmentation-free implantation of NPs fabricated in the gas phase. Surfactant-free silver NPs are generated in magnetron cluster sources,[16,17] where silver atoms are sputtered from a wire or disk target. The atomic vapor is quenched in an argon/helium atmosphere, promoting aggregation into NPs, a large fraction of which are positively charged. The whole cluster source is electrically floating with respect to ground, its potential defining the kinetic energy of the silver cluster ions. Time-of-flight mass spectrometry permits *in situ* monitoring and adjusting the mean particle size and dispersion. The beam is then focused onto the sample holder. In this study, NPs with mean diameter controlled between 2 and 5 nm are implanted at kinetic energies between 100 and 250 eV.

LbL films with two polyelectrolyte couples were deposited on quartz substrates by sequential dipping.[18] Two different polyelectrolyte couples are used here. Poly(allylamine hydrochloride) (PAH) and poly(sodium 4-styrenesulfonate) (PSS) in $(PAH/PSS)_n$ architecture is a standard system, the films described here typically consist of 150 bilayers with a total thickness of ∼300 nm. The second system used is polyethylenimine (PEI) and poly(acrylic acid) (PAA) in $(PEI/PAA)_n$ architecture, which has been shown to grow exponentially.[19] Here films of thickness ∼400 and ∼3200 nm were grown, corresponding to 3 and 4 bilayers, respectively. The materials were obtained from Sigma-Aldrich and used as received. All solutions were prepared in ultrapure water from a Sartorius Arium Comfort system. PAH and PSS solutions were prepared at 0.5 mg/ml, with the pH adjusted to 7 using 0.1 M HCl or 0.1 M NaOH solutions. The PEI solution was prepared at 1 mg/ml and pH 9, the PAA solution was prepared at 3 mg/ml and pH 3. The absence of degradation when transferring the films into vacuum was verified with optical absorption and Raman spectroscopy; in no case was a significant change in the response evidenced. Both film materials are very soft; a fragmentation-free particle penetration is expected even for the comparably low kinetic energies of ∼0.1 eV/atom.[8] The mean penetration depth is defined by the particle material, its size, and kinetic energy, as well as by the nature of the polymer material. We do not present a comprehensive quantification of the different parameters but rather demonstrate the principal feasibility of controlled NP dispersion in the polymer matrix. As the NP beam is focused onto the polymer film, the concentration of NPs continuously varies from the center of the deposition spot toward the edge of the film, permitting concentration dependent measurement series. Optical spectroscopy was performed in a Perkin Elmer Lambda 900 spectrophotometer in transmission mode. Where indicated linear polarizers were used. All spectra were normalized to reference spectra taken for undoped polymer films, outside the NP spot.

It is well known that, with increasing concentration, inter-particle coupling between neighboring NPs leads to a gradual redshift of the LSPR, transforming the optical response from the superposition of many individual NP LPSR signals to a collective response.[20,21] We have observed this behavior in many samples and spectroscopic geometries. While for weak coupling the (perturbed) LSPR is the spectroscopic fingerprint of choice, for higher metal loadings a simple spectroscopic response is not easily available. In the following, we will introduce a purely plasmonic characterization technique that covers the whole range of interest.

Interestingly, when performing the optical spectroscopy with linearly polarized light (TM) at an oblique angle (55° with respect to the surface normal for all spectra shown), i.e., with a component of the electrical field normal to the surface, an additional, narrow peak appears in the UV for many samples, as shown in Fig. 1. This peak is absent for highly dilute samples (e.g., Ag NPs in silica[22]) but it was observed for many different particle concentrations and different polymer matrices. It is observed up to highest Ag loading when the films start to turn opaque and mirror-like. At this point the LSPR is no longer measurable. The spectral position and width of this additional signal vary slightly between samples and illuminated spots but to a much lesser extent than the LSPR, which is red-shifted and broadened due to inter-particle interactions. When measuring in the same geometry but with TE polarized light or at perpendicular incidence, only the (red-shifted) LSPR remains and the additional peak in the UV disappears, as shown in Fig. 2. Here the relative shift of the TM LSPR with respect to the TE and perpendicular measurements may be

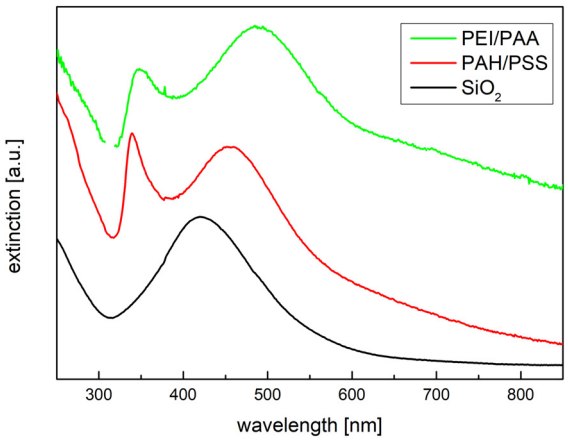

FIG. 1. Optical extinction spectra of Ag NPs in different matrices under TM irradiation. Strongly diluted particles in silica only show the well-known LSPR at 420 nm and the rise below ∼310 nm due to interband transitions[22] (black curve). Samples with higher concentrations in two different polymer matrices display a red-shifted LSPR and an additional peak around ∼340 nm, absent at TE illumination. NP diameters were 2.7 nm (SiO_2), 4.9 nm (PAH/PSS) and 2.2 nm (PEI/PAA).

attributed to the formation of anisotropic NP agglomerates but is not central to our argument. Slight variations between curves taken for different geometries are due to the different normalizations. Great care has been taken to ensure that the effects discussed in this Letter are independent of and much stronger than these normalization-dependent variations. Note that no size-dependent shifts of the intrinsic LSPR wavelength are expected for Ag NPs in comparable matrices.[22] The underlying mechanism responsible for the additional peak in the UV thus must be independent of the matrix and different from the LSPR.

We now show that the additional signal at ∼340 nm stems from the formation of a continuous thin silver film in the polymer matrix by comparing the samples described above to evaporated silver films. Structural information about the samples is presented in the supplementary material. In the case of a continuous silver thin film, a transmission window around 330 nm is well known and best seen in the red curve of Fig. 3. This (negative in extinction) peak is a particularity of silver and appears because of the very close energetic proximity of the volume plasma energy (3.75 eV) and the onset of interband transitions (IB) at ∼3.8 eV. A continuous Ag film efficiently reflects light below the plasma frequency but, contrary to simple Drude-type metals, the film then does not become transparent but the IB transitions start absorbing. Between these two regimes lies a narrow window of very high transmittance at approximately the volume plasma frequency,[23,24] depending on the exact nature of the film.

A silver film of thickness less than the skin depth can furthermore support several different plasmon modes, the best known being the Surface Plasmon Polaritons (SPP) in their short- and long-range version.[25] But there also exists a localized plasmon very close around the volume plasmon frequency.[26] Here the entire electron density oscillates perpendicular to the surface, comparable to a plane capacitor. These "normal surface plasma oscillation" or Ferrell modes[27,28] possess an oscillating dipole moment and thus couple directly to light, contrary to both longitudinal volume plasmons and plasmon polaritons. In fact Ferrell modes are the stationary counterpart of the long range propagative plasmon polariton in thin films, on the left side of the light line.[26] They can, however, only be excited with TM

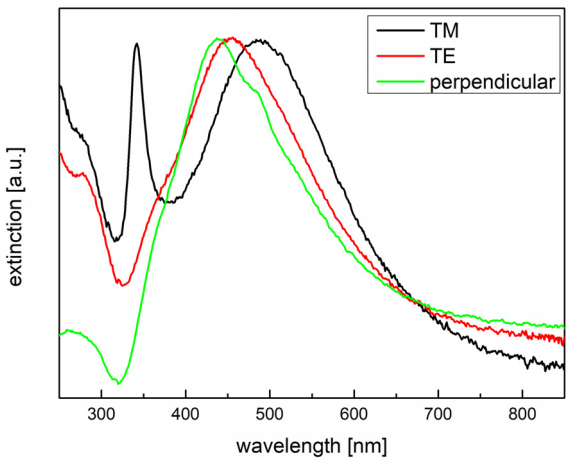

FIG. 2. Polarization dependence of the optical response for a sample with 3.5 nm Ag NPs in a PAH/PSS LbL film of ∼300 nm thickness.

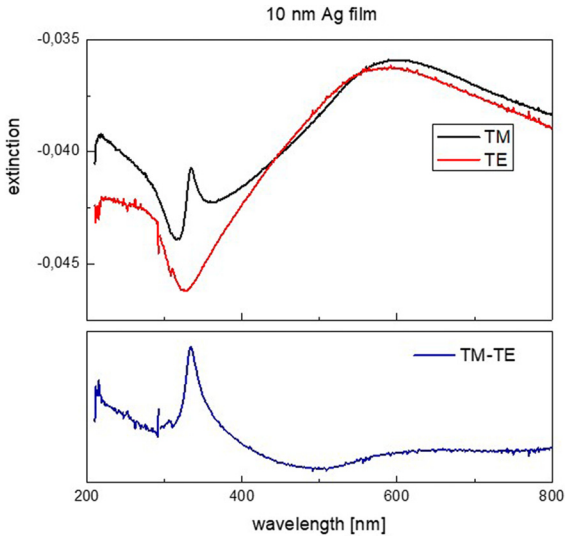

FIG. 3. Polarization dependence of the optical response for a thin Ag film of nominal thickness 10 nm. The blue curve is the difference between the TM and TE curves.

polarization, i.e., with a non-negligible component perpendicular to the thin film surface. This polarization dependence is shown for a 10 nm thick Ag film in Fig. 3. The difference curve in blue clearly shows the Ferrell plasmon resonance at 334 nm, i.e., at the plasma frequency of bulk silver. This Ferrell mode has been largely forgotten in the plasmonics community, except for a small number of publications based on its infrared counterpart (termed Berreman mode) in epsilon-near-zero materials.[29–31] Note that while closely related to, a Ferrell mode is neither a volume plasmon nor an SPP, none of which can be directly excited by light.

On this basis, we can now interpret the optical spectra of our cluster-assembled nanostructures. At lowest NP concentration, the intrinsic LSPR is measured. Its spectral position can be described by classical Mie theory taking into account the dielectric properties of the matrix and corrections due to quantum effects at the small sizes investigated here (<5 nm).[22] For larger particles, retardation and multipole excitations have to be considered.[20] Increasing the volume concentration to >5% results in inter-particle coupling and a consecutive redshift and broadening of the LSPR. Around the percolation, a more or less continuous thin silver film is formed and the Ferrell mode appears in TM geometry. The fact that the films are not homogeneous in thickness and possibly discontinuous only slightly broadens and shifts the Ferrell mode. We can, thus, use the plasmonic response of NP doped films to monitor coupling and agglomeration through the whole range from isolated NPs to continuous films. The second transition, from coupled NPs to the thin film, is demonstrated in Fig. 4, which shows TM and TE spectra at two different positions of a sample of 3.4 nm Ag NPs implanted into a $(PAH/PSS)_{150}$ LbL film. A deposition energy of 240 eV results in high spatial dispersion. At low particle density, only the LSPR of interacting Ag NPs is visible at ∼450 nm at the edge of the area with implanted NPs. Toward the center of the NPs spot the Ferrell plasmon peak appears in TM geometry.

The LSPR energy and width strongly depend on the shape and environment of the NP in question, thereby justifying their use in

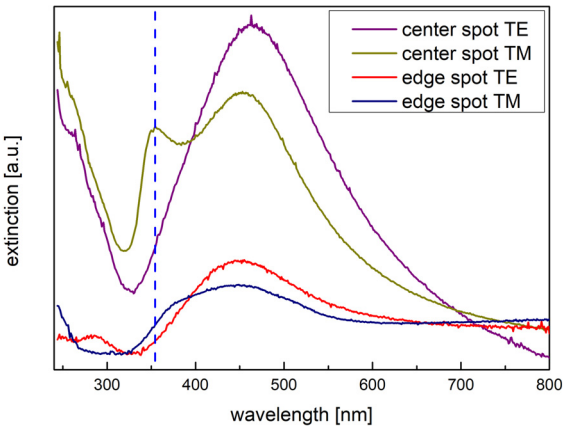

FIG. 4. Polarization-dependent plasmonic response curves of a sample with 3.4 nm Ag NPs implanted into a $(PAH/PSS)_{150}$ LbL film at a deposition energy of 240 eV. Only at high NP concentration, inside the particle spot, is the Ferrell plasmon of a continuous film visible.

sensing applications. The Ferrell mode, on the other hand, is much more insensitive to the local structure. Even comparably ill-defined nanostructured films, like the concentrated ones discussed here, show clear peaks with only slight shifts and broadening. This makes the Ferrell mode a simple fingerprint, easy to realize and measure in various types of nanostructure geometries, especially when compared to more complex optical techniques relying on hot spots or near field excitation.[32,33] Significantly, it does not require specific coupling through a high-index prism, as do the propagative surface plasmon polaritons.[34] A comprehensive theoretical description of the Ferrell mode in analogy to Refs. 29, 35, and 36, and in particular, for non-ideal systems like the ones presented here, is clearly desirable, but beyond the scope of this Letter.

In conclusion, we have shown that the loading of transparent thin films, here LbL fabricated polymer films, with silver nanoparticles, can easily be monitored by plasmon spectroscopy. Depending on the coupling between particles and their agglomeration into continuous metal film structures, a signal in the UV, additional to the well-known localized surface plasmon resonance, appears if a significant fraction of the electric field of the exciting light is normal to the film. This effectively forgotten Ferrell mode, at the volume plasmon frequency, is a fingerprint of a (semi-) continuous thin silver film, easy to realize and detect. Our wide-range plasmonic characterization technique is an important step toward the controlled tuning of nanoparticle doped polymer films for applications in sensors or fuel cell membranes.

See the supplementary material for the complementary structural characterization of thin Ag films and Ag NP doped LbL films.

The authors are grateful to the São Paulo Research Foundation (Nos. FAPESP 2014/03691-7, 2013/14262-7, and 2016/12807-4), CNPq, CAPES, and the Brazilian Science Without Borders "Special Visiting Scientist" Program (No. 88881.030488/2013-01) for financial support. Experimental support from the Microfabrication Laboratory of the Brazilian Nanotechnology National Laboratory (Nos. DB-C1-25094 and TEM-C1-25093) is acknowledged. This work was partly performed using the Lyon Cluster Research Platform PLYRA. We thank A. Piednoir, O. Boisron, C. Albin, and C. Clavier for technical support and J. Bellessa for fruitful discussions.

REFERENCES

[1]J. J. Richardson, M. Björnmalm, and F. Caruso, Science **348**(6233), aaa2491 (2015).
[2]J. A. Rogers, T. Someya, and Y. Huang, Science **327**, 1603 (2010).
[3]C. Pang, C. Lee, and K.-Y. Suh, J. Appl. Polym. Sci. **130**, 1429 (2013).
[4]K. R. Berry, Jr., A. G. Russell, P. A. Blake, and D. K. Roper, Nanotechnology **23**, 375703 (2012).
[5]J. Ferreira, F. S. Teixeira, A. R. Zanatta, M. C. Salvadori, R. Gordon, and O. N. Oliveira, Phys. Chem. Chem. Phys. **14**, 2050 (2012).
[6]O. N. Oliveira, R. M. Iost, J. R. Siqueira, F. N. Crespilho, and L. Caseli, ACS Appl. Mater. Interfaces **6**, 14745 (2014).
[7]T. Maurer, J. Marae-Djouda, U. Cataldi, A. Gontier, G. Montay, Y. Madi, B. Panicaud, D. Macias, P.-M. Adam, G. Lévêque, T. Bürgi, and R. Caputo, Front. Mater. Sci. **9**, 170 (2015).
[8]C. Ghisleri, F. Borghi, L. Ravagnan, A. Podestà, C. Melis, L. Colombo, and P. Milani, J. Phys. D: Appl. Phys. **47**, 015301 (2014).
[9]C. Gabriele, G. Cristian, M. Mattia, M. Paolo, and R. Luca, Adv. Mater. **23**, 4504–4508 (2011).
[10]C. Minnai and P. Milani, Appl. Phys. Lett. **107**(7), 073106 (2015).
[11]Y. Yunsong, S. Tommaso, B. L. Giacomo, M. Chloé, B. Andrea, P. Riccardo, D. Ilaria, F. Gabriele, M. Marco, L. Cristina, and M. Paolo, Adv. Mater. **29**, 1606109 (2017).
[12]V. N. Popok, C. M. Jeppesen, P. Fojan, A. Kuzminova, J. Hanuš, and O. Kylián, Beilstein J. Nanotechnol. **9**, 861 (2018).
[13]A. Riul, Jr., C. A. R. Dantas, C. M. Miyazaki, and O. N. Oliveira, Jr., Analyst **135**, 2481 (2010).
[14]M. M. Barsan and C. M. Brett, Trends Anal. Chem. **79**, 286– 296 (2016).
[15]L. A. Mercante, V. P. Scagion, A. Pavinatto, R. C. Sanfelice, L. H. C. Mattoso, and D. S. Correa, J. Nanomater. **2015**, 890637.
[16]M. Hillenkamp, G. Di Domenicantonio, and C. Félix, Rev. Sci. Instrum. **77**, 025104 (2006).
[17]A. D. T. de Sá, V. T. A. Oiko, G. di Domenicantonio, and V. J. Rodrigues, J. Vac. Sci. Technol., B **32**, 061804 (2014).
[18]R. C. Hensel, K. L. Rodrigues, V. D. L. Pimentel, A. Riul, and V. Rodrigues, MRS Commun. **8**, 283–288 (2018).
[19]J. Fu, J. Ji, L. Shen, A. Küller, A. Rosenhahn, J. Shen, and M. Grunze, Langmuir **25**(2), 672–675 (2009).
[20]U. Kreibig and M. Vollmer, *Optical Properties of Metal Clusters*, Springer Series in Materials Science (Springer Berlin, 1995).
[21]M. Quinten, *Optical Properties of Nanoparticle Systems* (Wiley-VCH, 2011).
[22]A. Campos, N. Troc, E. Cottancin, M. Pellarin, H.-C. Weissker, J. Lermé, M. Kociak, and M. Hillenkamp, Nat. Phys. **15**, 275–280 (2019).
[23]H. Ehrenreich and H. R. Philipp, Phys. Rev. **128**, 1622–1629 (1962).
[24]H. Ehrenreich, IEEE Spectrum **2**(3), 162–170 (1965).
[25]H. Raether, *Surface Plasmons on Smooth and Rough Surfaces and on Gratings* (Springer, 1988), pp. 4–39.
[26]R. Ritchie, Surf. Sci. **34**(1), 1–19 (1973).
[27]R. A. Ferrell, Phys. Rev. **111**, 1214–1222 (1958).
[28]A. J. McAlister and E. A. Stern, Phys. Rev. **132**, 1599–1602 (1963).
[29]S. Vassant, J.-P. Hugonin, F. Marquier, and J.-J. Greffet, Opt. Express **20**(21), 23971–23977 (2012).
[30]W. D. Newman, C. L. Cortes, J. Atkinson, S. Pramanik, R. G. DeCorby, and Z. Jacob, ACS Photonics **2**(1), 2–7 (2015).
[31]N. C. Passler, I. Razdolski, D. S. Katzer, D. F. Storm, J. D. Caldwell, M. Wolf, and A. Paarmann, ACS Photonics **6**, 1365–1371 (2019).
[32]K. Seal, D. Genov, A. Sarychev, H. Noh, V. Shalaev, Z. Ying, X. Zhang, and H. Cao, Phys. Rev. Lett. **97**(20), 206103 (2006).
[33]N. J. Borys, E. Shafran, and J. M. Lupton, Sci. Rep. **3**, 2090 (2013).
[34]A. Berthelot, G. C. des Francs, H. Varguet, J. Margueritat, R. Mascart, J.-M. Benoit, and J. Laverdant, Nanotechnology **30**, 015706 (2019).
[35]J. J. Burke, G. I. Stegeman, and T. Tamir, Phys. Rev. B **33**, 5186–5201 (1986).
[36]P. Berini, Phys. Rev. B **63**, 125417 (2001).